

Localization on a two-channel model with cross correlated disorderR.C.P. Carvalho, M.L. Lyra and F. A. B. F. de Moura
*Instituto de Física, Universidade Federal de Alagoas, 57072-970 Maceió, AL, Brazil*F. Domínguez-Adame
Departamento de Física de Materiales, Universidad Complutense, E-28040 Madrid, Spain

We study the wave-packet dynamics in a two-channel Anderson model with correlated diagonal disorder. To impose correlations in the disorder distribution we construct the on-site energy landscape following both symmetry and antisymmetric rules. The dynamics of an initially localized wave packet is investigated by solving numerically the time-dependent Schrödinger equation. Our numerical data show that symmetric cross correlations have a small impact on the degree of localization of the one-particle eigenstates. In contrast, antisymmetric correlations lead to an effective reduction of the effective degree of disorder, specially in the strong coupling regime, thus resulting in a substantial increase of the wave-packet spread. A finite size scaling analysis shows that the antisymmetric cross correlations, in spite of weakening the localization, do not promote ballistic transport. Theoretical explanations to the effect of cross-correlations in the wave-packet dynamics are provided.

PACS numbers: 78.30.Ly; 71.30.+h; 73.20.Jc

I. INTRODUCTION

The wave-packet dynamics in low-dimensional system is one of the main focus of the Anderson localization theory. By using perturbation theory and scaling analysis it was predicted the absence of extended eigenstates in low-dimensional systems with uncorrelated disorder [1]. Therefore, at long time the width of the time-dependent wave-packet localizes in a finite region around the initial position. More recently, it has been shown that low-dimensional disordered systems can support extended states or a localization-delocalization transition in the presence of short or long-range correlations in the disorder distribution [2–16]. The effect of long-range correlated scatters on the transport properties of microwave guides was experimentally studied and corroborated the predicted presence of mobility edges [16]. Moreover, it was suggested that an appropriate algorithm for generating random correlated sequences with desired mobility edges could be used in the manufacture of filters for electronic and optical signal processing [8].

The wave-packet dynamics in two-dimensional or multi-channel systems with correlated disorder is still an open issue with several connections to DNA geometries, semiconductors and superlattices. Particularly, the simple problem of the electron dynamics in two-channel structures has been the focus of several works [17–21]. The well known random dimer model [2] was generalized to the ladder case and a delocalized state at the band center was obtained [17]. Recently, an instructive debate about the possible existence of extended states in DNA-like two-channel models has emerged [19–21]. By using numerical calculations of the inverse participation ratio it was claimed that a two-channel model based on DNA segments could support extended states. [19]. Fur-

thermore, on the basis of group theory arguments, it was proved that single or double channel models need long-range correlations in the disorder distribution to display extended states [20]. Moreover, by using a perturbation theory [21], it was obtained a general formula for the localization length as a function of the autocorrelations along each channel and also the cross correlations between the channels. In agreement with Ref. [20], it was proved that extended states cannot appear solely due to cross correlations (e.g. DNA base paring). This discussion shows that the existence of extended states in two-channel model or DNA-like model is still an open question.

More recently, it was showed that a quasiperiodic two-chain model can support extended states at multiple values of the Fermi energy [22]. Further, it was demonstrated analytically that a two-channel random model can display a band of Bloch-type extended states when the on-site potentials and the hopping amplitudes display a particular correlation [23]. In Ref. [24] the effects of the coexistence of localized and extended states in the correlated random ladder model were investigated. By using numerical diagonalization and high-order methods to solve the Schrödinger equation it was shown that stationary and dynamical properties are dominated by extended states. In addition, it was numerically demonstrated that the superposition of localized and delocalized bands gives rise to a new level-spacing distribution [24].

The aim of the present work is to contribute to the understanding of the electronic wave-packet dynamics in a ladder geometry with correlated disorder. We impose cross correlations in the disorder distribution by introducing symmetry and antisymmetric rules between the on-site energy of each channel. The dynamics of an initially localized wave packet is investigated by numerically

solving the time-dependent Schrödinger equation. Our numerical data show that while symmetric cross correlations have a small influence on the degree of localization, antisymmetric cross correlations increase the wave-packet spread. A finite size scaling analysis shows that antisymmetric cross correlations, in spite of weakening the localization, do not promote ballistic transport. Theoretical explanations to the effect of cross correlations in the wave-packet dynamics are provided.

II. MODEL AND NUMERICAL PROCEDURE

Our calculations make use of an effective tight-binding model Hamiltonian which describes the dynamics of an electron in a ladder geometry with correlated disorder. Considering a single orbital per site and nearest-neighbor interactions, the time dependent Schrödinger equation (with $\hbar = 1$) is given by [20]

$$i \frac{d\psi_j^s}{dt} = \epsilon_j^s \psi_j^s + V_{||} (\psi_{j+1}^s + \psi_{j-1}^s) + V_{\perp} \psi_j^{\bar{s}}. \quad (1)$$

Here $s = \pm 1$ labels each strand of the ladder, and $\bar{s} = -s$ indicates its complementary. The index $j = 1, \dots, N$ runs over the sites along one of the strands, coupled by the hopping parameter $V_{||}$. V_{\perp} is the hopping parameter between complementary sites on each strand. The on-site cross correlated energies ϵ_j^s will be generated as follows: ϵ_j^{+1} will be chosen as an uncorrelated random sequence with $\langle \epsilon_j^{+1} \rangle = 0$ and uniformly distributed within $[-W, W]$; The on-site energy of the another channel will be chosen as (a) $\epsilon_j^{-1} = \epsilon_j^{+1}$ or (b) $\epsilon_j^{-1} = -\epsilon_j^{+1}$. These distinct symmetry rules impose, respectively, symmetric and antisymmetric cross correlations within the two-channel Hamiltonian.

We consider an electron initially localized at the orbital $|j_0 s_0\rangle$, namely we take the initial condition $\psi_j^s(t=0) = \delta_{jj_0} \delta_{ss_0}$. The set of equations above were solved numerically by using a high-order method based on the Taylor expansion of the evolution operator $V(\Delta t) = \exp(-iH\Delta t) = 1 + \sum_{l=1}^{n_o} (-iH\Delta t)^l / (l!)$, where H is the Hamiltonian. The wave-function at time Δt is given by $|\Phi(\Delta t)\rangle = V(\Delta t)|\Phi(t=0)\rangle$. The method can be used recursively to obtain the wave-function at time t . To obtain $H^l |\Phi(t=0)\rangle$ we will use a recursive formula. As a first step, we define $H^l |\Phi(t=0)\rangle = \sum_{j,s} (C_j^s)^l |j, s\rangle$. Using the Schrödinger equation (1) we can compute $H^1 |\Phi(t=0)\rangle$ and obtain $(C_j^s)^1$ as

$$(C_j^s)^1 = \epsilon_j^s \psi_j^s + V_{||} (\psi_{j+1}^s + \psi_{j-1}^s) + V_{\perp} \psi_j^{\bar{s}}. \quad (2)$$

Therefore, using that $H^l |\Phi(t=0)\rangle = H \sum_{j,s} (C_j^s)^{l-1} |j, s\rangle$, $(C_j^s)^l$ can be obtained recursively as

$$(C_j^s)^l = \epsilon_j^s (C_j^s)^{l-1} + V_{||} [(C_{j+1}^s)^{l-1} + (C_{j-1}^s)^{l-1}] + V_{\perp} (C_j^{\bar{s}})^{l-1}. \quad (3)$$

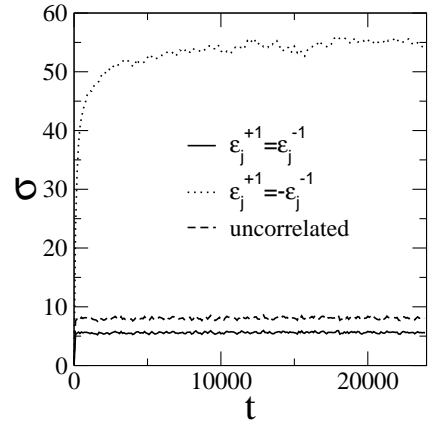


FIG. 1: The time-dependent wave packet width σ versus time t . Calculations were done using $N = 4000$ and considering distinct kinds of cross correlations within diagonal disorder. Antisymmetric cross correlations $\epsilon_j^{-1} = -\epsilon_j^{+1}$ lead to a wave packet width much larger than that one produced by symmetric cross correlations $\epsilon_j^{-1} = \epsilon_j^{+1}$.

Results were obtained by using $\Delta t = 0.5$ and the sum was truncated at $n_o = 20$. This cutoff was sufficient to keep the wave-function norm conservation along the entire time interval considered. This formalism is faster than high order Runge Kutta methods and it is easier to implement. Further details about the numerical formalism can be found in [25]. We are particularly interested in the square root of the mean-square displacement $\sigma(t)$ defined by

$$\sigma(t) = \sqrt{\sum_{j,s} [(j - j_0)^2 + (s - s_0)^2] |\psi_j^s(t)|^2}. \quad (4)$$

The mean-square displacement $\sigma(t)$ gives an estimate of the width of the wave packet at time t . In the long-time regime, its scaling behavior can also be used to distinguish between localized and delocalized wave packets [20]. In addition we compute the Lyapunov exponent $\gamma(E)$ (which is the inverse of the localization length Λ) of long two-channel segments, by means of the following equation:

$$\gamma(E) = 1/\Lambda(E) = (1/2N) \ln \left[\text{Tr} \left| G_{1,N+1}^{N+1} \right|^2 \right], \quad (5)$$

where $G_{1,N+1}^{N+1}$ denotes the Green's function operator between the first and the $(N+1)$ th pair of sites. To compute this operator, we use a standard recursion method (see Ref. [26] for details). For extended states, $1/\Lambda(E)$ vanishes in the thermodynamic limit.

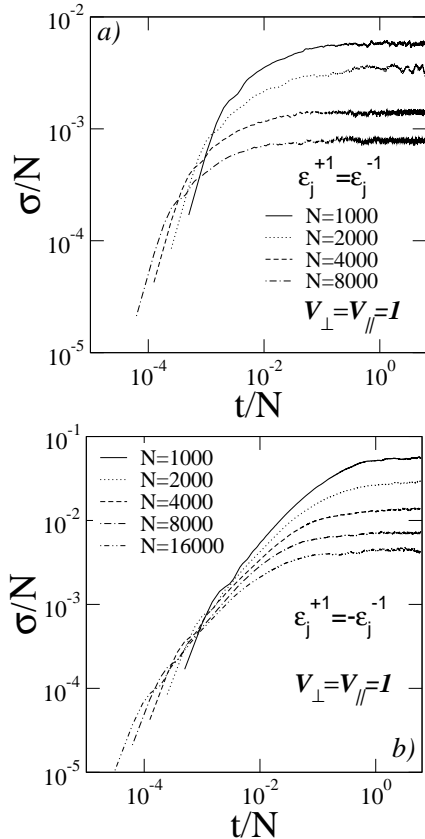


FIG. 2: Scaled wave packet width σ/N versus scaled time t/N . Calculations were done using $V_{\parallel} = V_{\perp} = 1$ and $N = 1000$ up to 16000 sites. Our calculations indicate that for both cross correlations used here, the asymptotic scaled wave packet width $\sigma/N \rightarrow 0$ as N increases, a typical signature of localized wave packets.

III. RESULTS

The numerical solution of the time dependent Schrödinger equation was performed on two-channel systems with $N = 1000$ up to 16000 sites on each strand. Numerical convergence was ensured by conservation of the norm of the wave-packet at every time step, i.e., $|1 - \sum_{js} |\psi_j^s(t)|^2| < 10^{-10}$. All calculations were averaged over 30 disorder configurations. In Fig. 1 we plot the time dependent wave packet width σ versus time t computed using $N = 4000$ sites, $V_{\parallel} = V_{\perp} = 1$, both kinds of cross correlations and a standard uncorrelated random two-channel system. We can see that antisymmetric cross correlations $\epsilon_j^{-1} = -\epsilon_j^{+1}$ (see dotted-line) display a localization degree much weaker than the other cases (see solid-line data for $\epsilon_j^{-1} = \epsilon_j^{+1}$ and dashed line for the uncorrelated case). In Fig 2 we offer a comparative numerical analysis between both types of cross correlations by considering the scaled wave packet width σ/N versus scaled time t/N . Calculations were done using

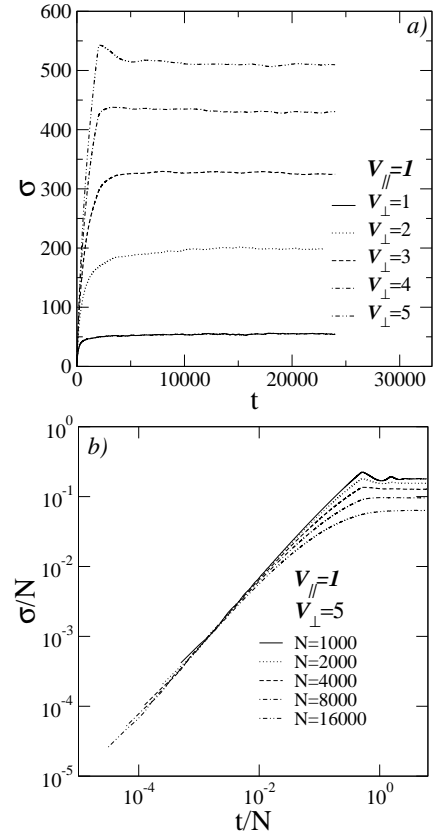


FIG. 3: (a) The wave packet width $\sigma(t)$ versus time t for $N = 4000$, $\epsilon_j^{-1} = -\epsilon_j^{+1}$, $V_{\parallel} = 1$ and $V_{\perp} = 1$ up to 5. When the intra-chain hopping V_{\perp} is increased in two-channel systems with antisymmetric cross correlations $\langle \epsilon_j^{-1} + \epsilon_j^{+1} \rangle = 0$ the local effective disorder along the quasi-unidimensional system goes to zero thus increasing the localization length. (b) Scaled spread σ/N versus scaled time t/N for $V_{\parallel} = 1$, $N = 1000$ up to 16000 sites and $V_{\perp} = 1$ up to 5, and $N = 1000$ up to 16000 sites. In spite of the cross correlations favors the increase of the localization length, it does not lead to truly extended wave packets once $\sigma/N \rightarrow 0$ as N increases.

$V_{\parallel} = V_{\perp} = 1$ and $N = 1000$ up to 16000 sites. For extended states, data from distinct chain sizes would collapse into a single curve, signaling a ballistic transport ($\sigma \propto t$). In our case, both calculations show no data collapse. Further, the scaled asymptotic wave packet width decreases as the system size increases, pointing to an ultimate localization of the wave packet in the thermodynamic limit. Therefore, the cross correlations used here do not induce extended states. These results agree with previous calculations found in Refs. [20, 21], confirming that diagonal cross correlations are not sufficient to promote a metal-insulator transition in a two-channel disordered Hamiltonian.

However, it is clear in both Figs. 1 and 2 that antisymmetric cross correlation $\epsilon_j^{-1} = -\epsilon_j^{+1}$ leads to a wave packet spread much larger than the symmetric

case ($\epsilon_j^{-1} = \epsilon_j^{+1}$). Let us stress that antisymmetric cross correlation contains the same ingredients used in the generic DNA model studied in Ref. [19], i.e., when $\langle \epsilon_j^{-1} + \epsilon_j^{+1} \rangle = 0$. We will show additional data and theoretical arguments to unravel the origin of the substantial decrease of the degree of localization and the apparent phase transition found in Ref. [19] in the two-channel model with antisymmetric diagonal cross correlations.

Let us first analyze in closer detail the two-channel model with symmetric cross correlated disorder. The Hamiltonian model of an isolated dimer pair has eigen-energies given by $\epsilon_j \pm V_\perp$. In the regime of strong interchain coupling these two modes can not be efficiently mixed by the intrachain coupling. Therefore the system shall behave as two uncoupled random chains with energy offset given by $\pm V_\perp$ and the disorder strength is simply the one originally present in the on-site energies. Within this scenario, the degree of localization shall be similar to the one present in the system without cross correlations. On the other hand, the Hamiltonian model of an isolated dimer pair with antisymmetric diagonal terms has eigen-energies given by $\pm\sqrt{\epsilon_j^2 + V_\perp^2}$. In the regime of strong interchain coupling these can be written as $\pm V_\perp + \epsilon_j^2/2V_\perp$. Also in this case, these modes are not effectively mixed by the intrachain coupling and the system shall behave as two independent random chains. However, the effective disorder is rescaled. It becomes of the order of $1/V_\perp$. Recalling that the localization length in random chains is proportional to the square of the inverse disorder width, antisymmetric cross correlations shall have exponentially localized states whose localization length grows with V_\perp^2 in the regime of strongly coupled chains.

In order to corroborate the above picture, we will provide additional numerical data of the wave packet width, density of states and localization length of the energy eigenmodes for both models with cross correlated disorder, as well as for the two-channel model with uncorrelated disorder. In Fig. 3(a) we plot the wave packet width $\sigma(t)$ versus time t for $N = 4000$, antisymmetric cross correlations $\epsilon_j^{-1} = -\epsilon_j^{+1}$, $V_\parallel = 1$ and $V_\perp = 1$ up to 5. The results show that the wave-packet spread increases as the intra-chain coupling V_\perp is also increased. However, even in the regime of strong intra-chain coupling V_\perp , the asymptotic scaled spread σ/N decreases with the system size, indicating an ultimate localization in the thermodynamic limit. Let us stress again that the calculations in Ref. [19] were done by using a two-channel system with a strong intra-chain coupling $V_\perp > V_\parallel$. Therefore, the reduction on the degree of localization reported in Ref. [19] actually reflects the weakening of the effective disorder in the two-channel system with antisymmetric cross correlations and strong intra-chain hopping. However, this specific cross correlation does not promote the emergence of truly extended states. To further illustrate this point, we provide some results from the exact diagonalization of the present two-channel Hamiltonian models. We show in Fig. 4 the normalized density of states

($\text{DOS}(E) = \sum_{E_n} \delta(E - E_n)$ where E_n are the eigenvalues obtained from numerical diagonalization) versus energy E . Calculations were done using $N = 5000$ sites, 500 disorder configurations and $V_\parallel = 1$ and $V_\perp = 5$ [see Fig. 4(a) and 4(b)]. When the intrachain and interchain couplings are of the same order, the DOS displays a single band which start to split in a two band structure when the intrachain coupling is increased. We already notice that, even in this regime of intermediate intra-chain coupling, the band edges in the presence of antisymmetric cross correlations are sharper than in the other cases. For large intra-chain hopping the density of states of the two-channel systems with symmetric cross correlations is quite similar to the one displayed by the corresponding uncorrelated model. The DOS in these two cases resembles the one of two uncoupled chains with a finite disorder width, signaled by the rounding of the band edges. On the other hand, the DOS of the model with antisymmetric cross correlations displays quite sharp band edges in the limit of strong intrachain coupling which is consistent with the vanishing of the effective disorder.

In Fig. 5 we plot the localization length Λ versus energy E computed using $N = 10^7$ sites for both kinds of cross correlations and a standard uncorrelated random two-channel system. We consider $V_\parallel = 1$ and $V_\perp = 1$ and $V_\perp = 5$. Notice that, even in the regime of intermediate intrachain coupling, the localization length near the band edges is one order of magnitude larger in the presence of antisymmetric cross correlations when compared with the other two cases. This effect becomes much more pronounced in strongly coupled channels. In Fig. 5(c) we plot the larger localization length Λ_{max} versus the intra-chain hopping V_\perp . The localization length diverges as $(V_\perp)^2$ in two-channel systems with antisymmetric cross correlations, while symmetric cross correlations have a small influence on the degree of localization. These numerical results corroborate our theoretical arguments given above.

IV. SUMMARY AND CONCLUSIONS

In this work we revisited the problem of electronic wave packet dynamics in two-channel disordered structures. We considered an Anderson Hamiltonian in a quasi-unidimensional geometry (a two-channel geometry). In particular, we studied in detail two distinct types of two-channel models with cross correlations within the diagonal disorder. By following the time evolution of an initially localized wave-packet, we showed that quasi-unidimensional structures with diagonal disorder displaying local correlations do not support truly extended states. In addition, we showed that symmetric cross correlations ($\epsilon_j^{-1} = \epsilon_j^{+1}$) have a very limited influence on the degree of localization. In contrast, antisymmetric cross correlations ($\epsilon_j^{-1} = -\epsilon_j^{+1}$) substantially inhibit the Anderson localization, specially in the regime of strongly coupled chains. The physical mechanism underlying the

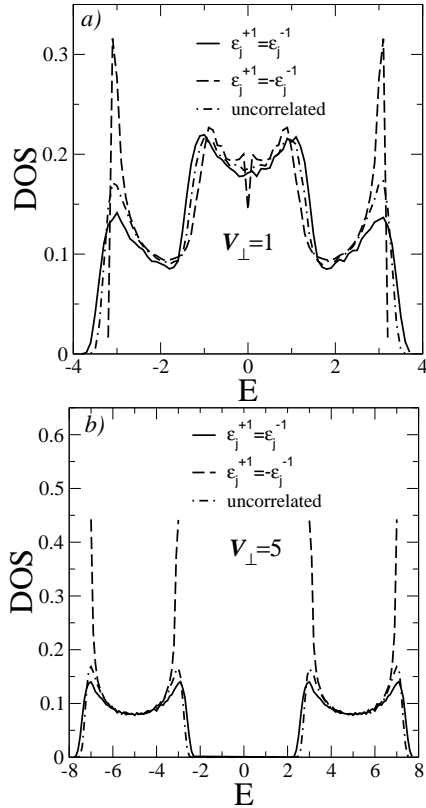


FIG. 4: (a) The normalized density of states $DOS(E)$ versus energy E computed using $N = 5000$ sites, 500 disorder configurations and (a) $V_{\perp} = 1$, (b) $V_{\perp} = 5$. When the intra-chain hopping V_{\perp} is increased in two-channel systems with antisymmetric cross correlations ($\epsilon_j^{-1} + \epsilon_j^{+1} = 0$), the density of states becomes similar to the DOS of two uncoupled perfect chains with on-site energies V_{\perp} and $-V_{\perp}$. Symmetric cross correlations produce a DOS with rounded band edges, signaling that the underlying disorder remains relevant even in the regime of strong intrachain coupling.

above phenomenology was revealed by stressing that, in the regime of strong interchain couplings, the energy eigenmodes can be roughly decoupled in those of two independent random chains with symmetric energy offsets. While symmetric cross correlations keep the strength of the effective disorder finite, antisymmetric cross correlations leads to a rescaled disorder width which vanishes as the interchain coupling increases. Such reduction of the effective disorder is reflected in the localization length of the energy eigenmodes, which can surpass 10^3 base pairs even for moderate interchain couplings. Therefore, these states behave as effectively extended in small

systems, leading to an apparent metal-insulator phase-transition [19].

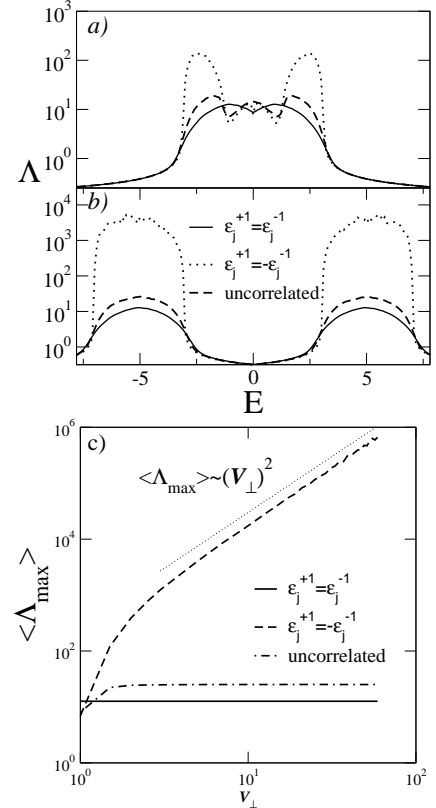


FIG. 5: (a,b) The localization length Λ versus energy E computed using $N = 10^7$ sites, both kinds of cross correlations and a standard uncorrelated random two-channel system. Calculations were done using $V_{\parallel} = 1$, (a) $V_{\perp} = 1$ and (b) $V_{\perp} = 5$. (c) The largest localization length Λ_{\max} versus intra-chain hopping V_{\perp} . The localization length diverges with $(V_{\perp})^2$ in two-channel systems with antisymmetric cross correlations while it remains finite in the other two cases.

V. ACKNOWLEDGMENTS

This work was partially financed by the Brazilian Research Agencies CAPES (PROCAD, Rede NanoBioestruturas), CNPq (INCT-Nano(Bio)Simes, Project no. 573925/2008-9) and FAPERN/CNPq (Pronex). Work at Madrid was supported by MEC (projects MOSAICO and MAT2010-17180). FABF de Moura would like to thank the hospitality of Departamento de Física de Materiales (UCM).

- [1] E. Abrahams, P. W. Anderson, D. C. Licciardello, and T. V. Ramakrishnan, Phys. Rev. Lett. **42**, 673 (1979).
 [2] D. H. Dunlap, H. L. Wu, and P. W. Phillips, Phys. Rev.

Lett. **65**, 88 (1990); H.-L. Wu and P. Phillips, *ibid.* **66**, 1366 (1991).

- [3] F. Domínguez-Adame, E. Maciá, and A. Sánchez, Phys.

- Rev. B **48**, 6054 (1993).
- [4] F. A. B. F. de Moura and M. L. Lyra, Phys. Rev. Lett. **81**, 3735 (1998).
- [5] F. A. B. F. de Moura, M. D. Coutinho-Filho, E. P. Raposo, and M. L. Lyra, Phys. Rev. B **66**, 014418 (2002).
- [6] F. A. B. F. de Moura, M. D. Coutinho-Filho, E. P. Raposo, and M. L. Lyra, Phys. Rev. B **68**, 012202 (2003).
- [7] F. Domínguez-Adame, V. A. Malyshev, F. A. B. F. de Moura and M. L. Lyra, Phys. Rev. Lett. **91** 197402 (2003).
- [8] F. M. Izrailev and A. A. Krokhin, Phys. Rev. Lett. **82**, 4062 (1999); F. M. Izrailev, A. A. Krokhin, and S. E. Ulloa, Phys. Rev. B **63**, 41102 (2001).
- [9] G. P. Zhang and S.-J. Xiong, Eur. Phys. J. B **29**, 491 (2002).
- [10] F. A. B. F. de Moura, M. D. Coutinho-Filho, E. P. Raposo and M. L. Lyra, Europhys. Lett. **66**, 585 (2004).
- [11] V. Bellani, E. Diez, R. Hey, L. Toni, L. Tarricone, G. B. Parravicini, F. Domínguez-Adame, and R. Gómez-Alcalá, Phys. Rev. Lett. **82**, 2159 (1999).
- [12] H. Shima, T. Nomura, T. Nakayama, Phys. Rev. B **70** 075116 (2004).
- [13] G. Schubert, A. Weiße and H. Fehske, Physica B **801** 359(2005).
- [14] W. S. Liu, T. Chen, and S. J. Xiong, J. Phys. Condens. Matter **11**, 6883 (1999).
- [15] F. A. B. F. de Moura, M. L. Lyra, F. Domínguez-Adame, and V. A. Malyshev, J. Phys.: Condens. Matter **19**, 056204 (2007).
- [16] U. Kuhl, F. M. Izrailev, A. Krokhin, and H. J. Stöckmann, Appl. Phys. Lett. **77**, 633 (2000).
- [17] T. Sedrakyan and A. Ossipov, Phys. Rev. B **70**, 214206 (2004).
- [18] L. Tessieri and F. M. Izrailev, J. Phys. A **39**, 11717 (2006).
- [19] A. Caetano and P. A. Schulz, Phys. Rev. Lett. **95**, 126601 (2005).
- [20] A. Sedrakyan and F. Domínguez-Adame, Phys. Rev. Lett. **96**, 059703 (2006); E. Díaz, A. Sedrakyan, D. Sedrakyan, and F. Domínguez-Adame, Phys. Rev. B **75**, 014201 (2007).
- [21] V. M. K. Bagci and A. A. Krokhin, Phys. Rev. B, **76** 134202 (2007).
- [22] S. Sil, S. K. Maiti, and A. Chakrabarti, Phys. Rev. Lett. **101**, 076803 (2008).
- [23] S. Sil, S. K. Maiti, and A. Chakrabarti, Phys. Rev. B **78**, 113103 (2008).
- [24] F.A.B.F. de Moura, R.A. Caetano, M. L. Lyra, Phys. Rev. B, **81**, 125104 (2010).
- [25] W. S. Dias, E. M. Nascimento, M. L. Lyra, and F.A.B.F. de Moura, Phys. Rev. B, **76**, 155124 (2007).
- [26] B. Kramer and A. MacKinnon, Rep. Prog. Phys. **56** 1469 (1993).